The International Archives of the Photogrammetry, Remote Sensing and Spatial Information Sciences, Volume XLVIII-2/W7-2024
Optical 3D Metrology (O3DM), 12–13 December 2024, Brescia, Italy

Using Hyperfocal Distance in Close-Range Photogrammetry for Indoor Modelling

Etienne Sommer[1], Mathieu Koehl[1], Pierre Grussenmeyer[1]

[1]Université de Strasbourg, INSA Strasbourg, ICube Laboratory UMR 7357, Photogrammetry and Geomatics Group, CNRS Strasbourg, France - (etienne.sommer, mathieu.koehl, pierre.grussenmeyer)@insa-strasbourg.fr

Commission II

Keywords: Hyperfocal distance, Indoor photogrammetry, Close-range photogrammetry, Mesh optimisation, 3D modelling, Medieval heritage.

Abstract

Photogrammetry has recently gained in popularity for surveying buildings and exterior structures, thanks in particular to the use of drones, terrestrial or aerial imagery, and other devices that allow quality images to be obtained with sufficient distance. These approaches are ideal for capturing exterior architectural details where space allows greater flexibility to take pictures. However, when it comes to indoor surveys, spatial constraints and limited distance make it difficult to acquire quality data. In confined spaces, control of depth of field becomes an essential parameter for obtaining sharp images, which are essential to generate accurate 3D models.
In this context, the hyperfocal distance is used and demonstrated as an effective approach for optimizing terrestrial and indoor photogrammetry. Hyperfocal distance enables depth of field to be maximised without the need for frequent optical adjustments or changes in position during shooting. This technique is particularly advantageous in limited spaces where recoil is difficult to adjust, thus avoiding constant intervention on lens parameters and enabling it to be properly calibrated. Thanks to this approach, it is possible to obtain a homogeneous sharpness on each shot, for elements at different distances, enhancing the accuracy of the data and the quality of the 3D models generated.
This method has been applied to the throne room at Trifels castle in Germany. By using the hyperfocal distance, complex details were captured on site, enabling optimized data processing afterward. The model obtained is compared with surveys carried out by laser scanners, both terrestrial and mobile, enabling to validate the accuracy and repeatability of this method in a heritage documentation and conservation context.
Finally, the various potential applications for the obtained data are explored, depending on the final objectives, whether for analysis or for display and communication to the general public. This processing and optimisation stage is part of an approach to enhance the value of built heritage, making old architectural elements accessible and understandable, while ensuring faithful digital conservation.

1. Introduction

The methods for documenting and modelling heritage sites have been widely studied, primarily using photogrammetry or laser scanning. Each method has its advantages and drawbacks, and while initially seen as competitors, recent studies have explored the potential of combining these techniques (Matoušková et al., 2021; Tsiachta et al., 2024).

However, modelling these sites can be complicated when the space is restricted or the lighting conditions are not optimal. In such cases, laser scanning offers the significant advantage of capturing scenes almost 360 degrees, with a minimum acquisition distance of a few tens of centimetres depending on the scanner used. Photogrammetry, in contrast, can be challenging due to its limited field of view compared to scanners. Yet, it is much more cost-effective: a few thousand euros for a good full-frame camera and quality optics, versus tens of thousands of euros for a laser scanner, whether static or dynamic. This study therefore aims to explore the potential use of photogrammetry and leverage the hyperfocal distance for documenting and visualizing the throne room of the Trifels castle in Germany, located in the Rhineland-Palatinate state.

This approach is implemented within the framework of the Interreg VI Project (2023-2025): "Châteaux Rhénans - Burgen am Oberrhein", a cross-border initiative involving France, Germany, and Switzerland, coordinated by the European Collectivity of Alsace. Specifically, our methodology aligns with Action 4.6 of the project, which focuses on the 3D valorisation of heritage sites, thereby providing a dynamic and innovative solution for digital heritage conservation and study.

2. Related Work

The use of laser scanning enables obtaining a dense, colorized point cloud with sub-centimetre accuracy under optimal acquisition conditions (Rapuca and Matoušková, 2023). Moreover, for confined spaces, it has the advantage of enabling acquisition in all directions, reducing time on site and simplifying acquisition processes (Jordá et al., 2011). Additional methods can be employed when even finer acquisitions are needed, such as with a ScanArm (Grussenmeyer et al., 2012), but due to implementation difficulties and the vast amount of data produced, this method is limited to small objects or areas. These processes are highly effective for surveys where geometric data quality is crucial, but they are extremely costly, typically tens of thousands of euros, whereas photogrammetry is much more cost-effective.

Processed data from photogrammetry are similar to those from laser scanning: dense point clouds and subsequent mesh generation are achievable (Pavelka et al., 2022). The difference lies primarily in acquisition and processing. Photogrammetric acquisition inherently follows the orientation of the camera

lens. Using a panoramic camera could be useful for capturing data in confined spaces (Covas et al., 2015; Barazzetti et al., 2017; Bruno et al., 2024), but subsequent photogrammetric processing is often challenging, yielding less satisfactory results than with a DSLR or mirrorless camera (Dlesk et al., 2019). Enclosed spaces typically have poor lighting conditions directly related to the room's geometry. Unlike laser scanning methods, these conditions are critical to ensure satisfactory photogrammetric results (Lluis i Ginovart et al., 2014; Caroti et al., 2018). Therefore, supplementary artificial lighting may be necessary to achieve consistent, neutral lighting across the entire object being studied (Pérez Ramos and Robleda Prieto, 2015). Moreover, close-range photogrammetry presents challenges related to the focus areas in each image. In cases where the focus is on an object at a short distance, it is typically a few metres or less. Kraus (2007) presents the mathematical principles related to sharp focus, with a section that pays particular attention to cases involving nearby objects. In extreme cases, achieving sharp focus over the entire object may require stacking photos with successive focus zones, a time-consuming method more suitable for small objects (Marčiš et al., 2016).

3. Methodology

3.1 Presentation of the case study

The Trifels castle, located in the commune of *Annweiler am Trifels* in *Rhineland-Palatinate*, Germany, was occupied from the XIIth to the XIVth century. The castle fell into ruin before being restored during the Second World War, who aimed to glorify Germany's imperial past rather than restore it to its original state (figure 1). This castle is part of the Interreg project, for which the current modelling serves both documentation and promotion purposes. The castle has undergone restorations, and its interior rooms are now open to visitors, significantly enhancing the site's appeal. Among these rooms is a large throne hall, which attracts numerous visitors. To document and also promote its value to the public, a digital visualization of this hall is presented in this study. Visual realism plays a critical role, as the model must be photorealistic to create an immersive experience for visitors. Therefore, photogrammetric methods were chosen, as they allow for high-resolution textures at a lower cost than using a laser scanner.

Figure 1. Overview of the Trifels (Pfeuffer, U., 2024)

This study specifically focuses on the Trifels throne hall, with approximate dimensions as follows:

- The first floor is a large, regular pentagonal room with an area of approximately 130 m^2 and a height of 11 metres. Two alcoves, each about 12 m^2 in size and 5 metres high, are connected to this main room.
- The second floor consists of a room connected to the first floor by a staircase. It measures approximately 35 m^2 with a height of 4 metres. Additionally, a very narrow corridor (less than 1 metre wide) allows for circulation around the first floor, offering a top view of it.

3.2 Determining the hyperfocal distance

All parts of the throne room must be captured to ensure accurate geometry and coherent textures. According to the room's configuration and size (figure 2), areas of interest can be both close to the camera and in the background in the same shot. Therefore, it is crucial to ensure that both areas are in focus simultaneously.

Figure 2. Trifels' throne room (Kulbe, E., 2024)

This is achieved by using the hyperfocal distance of the lens (Vujic et al., 2021), which is the shortest distance at which the lens can be focused while keeping objects at infinity sharp. This distance, given by relation (1), helps to adjust the lens focus to achieve the greatest possible depth of field, keeping everything from half this distance to infinity in sharp focus. Kingslake (1992); Kraus (2007) and Luhmann et al. (2014) present the development that allows the determination of this relationship based on the basic optical properties of a lens. Moreover, Stubbs (2021) and Spencer (2023) maintain photography-dedicated websites that include articles related to the use of hyperfocal distance, featuring excellent examples of practical application.

$$H = \frac{f^2}{N \cdot c} + f \tag{1}$$

where :

- H is the hyperfocal distance (in metres)
- f is the focal length of the lens (in metres)
- N is the aperture number (f-stop) (unitless)
- c is the circle of confusion (in metres)

3.3 Surveying method using hyperfocal distance

For this study, a *Canon EOS R5* camera was used, equipped with a lens having a fixed focal length of 28 millimetres. The circle of confusion value c is provided by the manufacturer and specific to the camera (0.035 millimetres for the *Canon EOS R5* used here (Canon, 2024)). Thus, only the value of N remains a

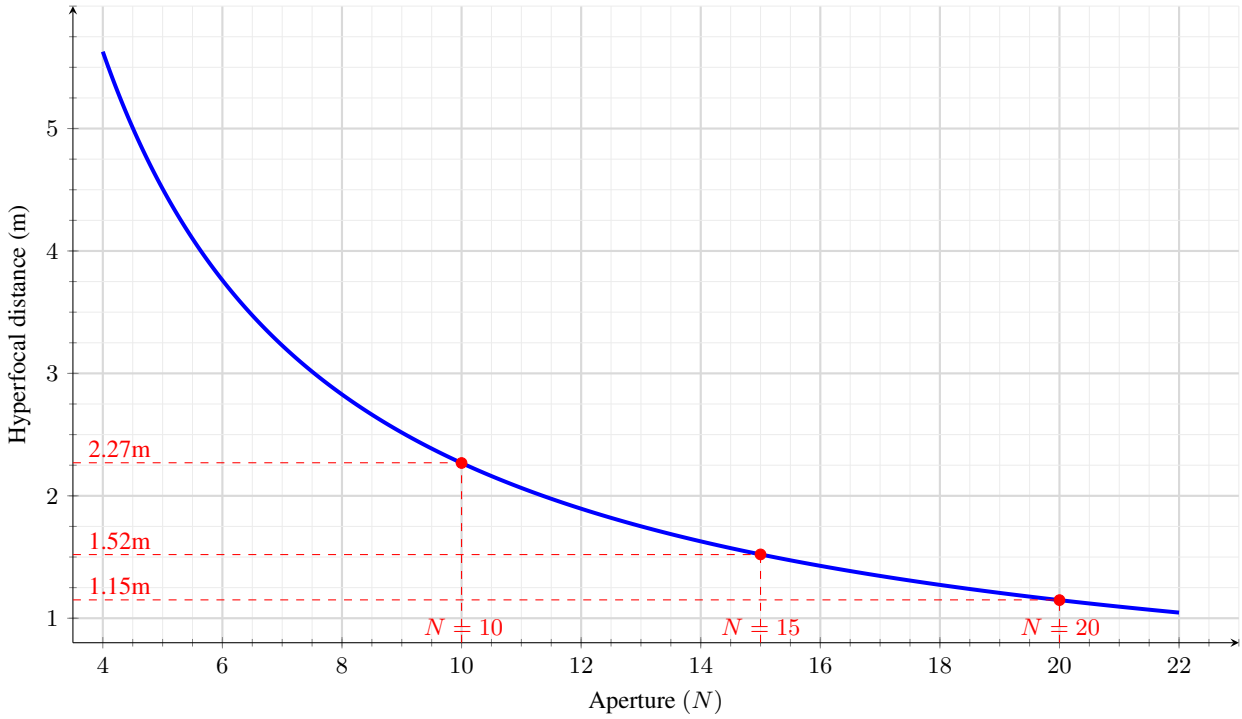

Figure 3. Hyperfocal distance as a function of N for focal length = 28 mm and for Canon EOS R5

parameter in the equation, allowing this value to vary to obtain different hyperfocal distances.

Figure 3 shows clearly that the relation (1) is not linear. The hyperfocal distance decreases rapidly at first, then more slowly. For confined spaces, an aperture of 20 was chosen, resulting in a hyperfocal distance of 1.15 metres. This ensures sharpness from 57.5 centimetres (half the hyperfocal distance) to infinity. The hyperfocal focusing was set before the acquisition of the first image and remained unchanged throughout the entire process. This consistency ensured a high number of photos with identical optical parameters, allowing for proper lens calibration.

However, setting a small aperture means less light reaches the sensor, resulting in darker images. There are three possible solutions to this problem:

- Brightly illuminate the room, which is not feasible as it is open to the public.
- Increase the ISO sensitivity.
- Increase the exposure time.

Increasing the ISO sensitivity adds noise to the image, degrading it. Therefore, the best solution was to increase the exposure time. To avoid motion blur, the camera was mounted on a tripod, and the photos were taken using a timer. This results in sharp images across all planes, without motion blur, and with minimal noise.

The main difficulty during data acquisition was related to the lighting conditions in the room. Large windows illuminated the space, causing significant issues when capturing images directed towards them. Some images ended up with completely overexposed areas, making it impossible to accurately determine the surfaces of objects in those zones. A potential solution to this issue could have been to create *HDR* images by combining multiple exposures but the on-site time constraints did not allow this method to be pursued. Some shooting angles were adjusted to optimize lighting; however, this was not feasible for areas directly adjacent to the windows.

3.4 Image alignment and project scaling

A total of approximately 600 images were acquired on-site over a period of about 3 hours. These images were then oriented using the Agisoft (2024) Metashape software. Since the room under study is entirely enclosed, only the scale of the room is important for the project, and not the georeferencing in a German coordinate system. To achieve this, metal scale bars with attached targets, whose distances were precisely measured using a total station during a master's project, were uniformly placed in the room. These targets were automatically detected by Metashape, allowing for more accurate target positioning than if done manually.

After the initial alignment, the tie points were analysed to remove those with the largest reprojection and precision errors, enabling the optimization of image alignment and camera calibration. The scale bars were distributed as either control scale bars or check scale bars, ensuring both categories were evenly spread throughout the room. The distance errors obtained were less than one millimetre across all measurements, regardless of their type, and the residuals for the camera calibration were on the order of one millimetre. These preliminary checks thus provide an initial validation of the proposed method.

3.5 3D reconstruction of the throne room

The 3D reconstruction via photogrammetry was performed using Agisoft Metashape. The mesh was generated using the depth maps of the images, consistently selecting *High* for both accuracy and the number of faces of the mesh. This resulted

in a complete scaled mesh of the throne room, with approximately 37 million faces. Aside from some images near the windows, as discussed in section 3.4, the colorimetry was consistent across the images. Consequently, the textures computed in Metashape and applied to the mesh were also uniform, allowing for a visually realistic representation of the scene. A more in-depth quantitative analysis of the mesh quality will be presented in section 4.2.

4. Analysis and evaluation of the photogrammetric mesh

To validate or not the presented method, it is essential to compare the photogrammetric mesh with data obtained from other surveying techniques. In this case, the comparison will be made with two types of data:

- *MMS* (Mobile Mapping System) data
- *TLS* (Terrestrial Laser Scanning) data

TLS data is known for its high geometric accuracy, but the acquisition process can be time-consuming. Conversely, the emergence of *MMS* allows for much shorter acquisition times, though with lower data quality. Comparing the photogrammetric data with these two methods is therefore crucial for both the quality of the data obtained through photogrammetry and the time efficiency, given the limited time available on-site.

4.1 Qualitative study of the photogrammetric mesh

4.1.1 First observations of the reconstruction: A preliminary qualitative study of the results seems appropriate, since visualizing the scene is one of the objectives of the study. At first glance, the results are very satisfactory. Fine details of the scene are visible, and the mesh exhibits minimal noise. The shapes and the scale of the objects are well preserved, with no noticeable drift or duality in the mesh. However, it should be noted that in more distant areas, such as the ceiling or the upper parts of the walls, the mesh is less detailed due to the increase of the *GSD*.

Some issues appear particularly around highly illuminated areas, such as lights and windows. Since these zones are sometimes overexposed in the photos, the quality of the mesh in these areas is significantly degraded. Only the general shape remains, but the details of the objects are lost. Moreover, as is common in most indoor surveys (whether by photogrammetry or *TLS*), objects such as furniture, lamps, and doors were not well reconstructed.

4.1.2 Comparison with the mesh obtained by *MMS*: The *MMS* survey was conducted using the *Faro Orbis*. The mesh reconstructed from the point cloud reveals immediate noise, with details that are less visible compared to those on the photogrammetric mesh. However, the survey was completed very quickly (in a matter of approximately 20 minutes), and the highly illuminated areas near the windows were better reconstructed. Additionally, the survey was easier to conduct in confined spaces, such as staircases or around the perimeter of the room.

4.1.3 Comparison with the mesh obtained by *TLS*: In contrast to *MMS*, the point cloud obtained by *TLS* is of very high quality. This point cloud was captured using the *Faro Focus Premium* with a flash survey, significantly reducing the time on-site by utilizing a *Ricoh Theta* camera and point interpolation (Sammartano et al., 2024). Here, the resulting mesh is fine, noise-free, and dense, allowing for the precise modelling of the scene's details. This method has the advantage of facilitating data acquisition, even near highly illuminated areas, but requires more time on-site.

4.2 Quantitative study of the photogrammetric mesh

The visual results of the reconstruction are encouraging, but it is necessary to quantify the data in order to have an objective and reliable comparison. To achieve this, the photogrammetric mesh is compared to the meshes obtained by *MMS* and *TLS*. These meshes were computed after an initial cleaning of the point clouds to remove outliers and noise. The reconstructions were performed in CloudCompare (2024) using the Poisson Reconstruction plugin (Kazhdan et al., 2006) with a fixed triangle size of 1 millimetre. Elements at different distances and with varying shapes were reconstructed to provide a comprehensive overview of both the strengths and limitations of the photogrammetric survey.

To enable comparison between the meshes, CloudCompare was also used. An initial rough alignment was done manually between the meshes to initialize the *ICP* (*Iterative Closest Point*) algorithm (Besl and McKay, 1992), which was then applied to achieve fine registration (taking care not to change the scale of the models). Once this alignment was completed, a mesh-to-point comparison was carried out. The main advantage of this method is that it provides signed distances, allowing for a detailed statistical analysis of the results.

4.2.1 Modelling of fine details: A sculpted stone at the base of a vault was surveyed to assess the modelling possibilities with the three methods. The focus here is on an object with fine details, positioned approximately 2 metres away during acquisition. The object measures about 1.2 metre in length, 0.4 metre in width, and 0.8 metre in height, while being positioned around 3 metres above the ground.

The results of the comparison are presented in table 1. All the values in the table are in metres, and the *ICP* value corresponds to the root mean square error of the *ICP* calculation between the 2 meshes. The results are very promising: the mean deviations are on the order of a millimetre, while the standard deviation (*std*) is a few millimetres. These deviations are illustrated in the histograms with figure 4. From this, it can be concluded that for elements acquired from a distance of a few metres, photogrammetric surveys with hyperfocal focusing yield very satisfactory results.

Reference	Compared	*ICP*	Mean	*Std*
TLS	*Orbis*	0.002	0.001	0.002
TLS	Photogrammetry	0.002	0.001	0.002
Orbis	Photogrammetry	0.002	0.000	0.003

Table 1. Sculpted stone comparison (metres)

However, during the qualitative analysis of the meshes, it was noted that the mesh from the *Orbis* survey is noisy and does not capture the fine details present in reality. These details are quite

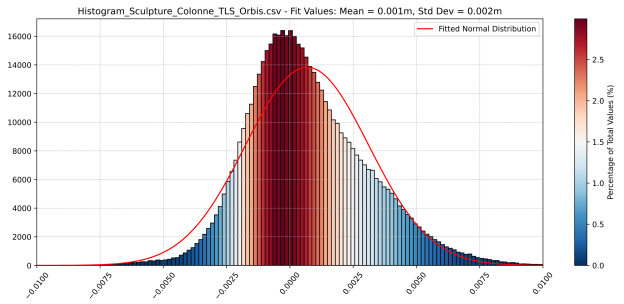

TLS-MMS comparison for a sculpted stone

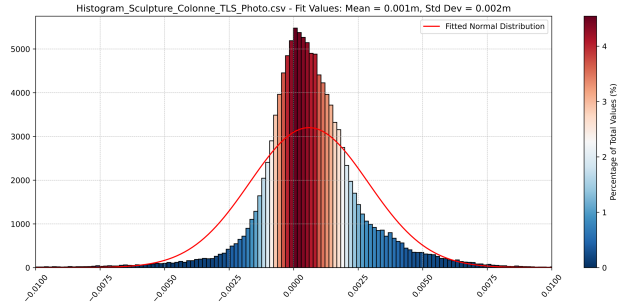

TLS-Photogrammetry comparison for a sculpted stone

Mesh obtained from *MMS* data

Mesh obtained from photogrammetric data

Figure 4. Sculpted stone comparison with a *TLS* as reference

subtle, at the noise threshold level, which is why this noise is not necessarily apparent in the above quantitative results. Nevertheless, the comparative results between *Orbis* and photogrammetry are of the same order as those with *TLS*. In some cases below, these two methods will be compared due to the unavailability of *TLS* data.

4.2.2 Modelling of the ceiling: The ceiling at the top of the room is located approximately 11 metres above the ground. Here, the benefit of using hyperfocal distance becomes evident: the same focus settings used to photograph the sculpted stone were also employed for capturing this structure. If necessary, both elements can be captured in the same shot without depth of field issues, allowing both areas to appear sharp.

In this case, no *TLS* data is available, so the *MMS* and photogrammetric data are directly compared. First, since the ceiling is further away and the focal length remains constant, the *GSD* size increases. A loss of detail in the model is therefore expected. The deviations between the two models (table 2 and figure 5) show that the average distance remains on the order of millimetres, but the standard deviation increases significantly.

Reference	**Compared**	***ICP***	**Mean**	***Std***
Orbis	Photogrammetry	0.021	0.002	0.013

Table 2. Roof comparison

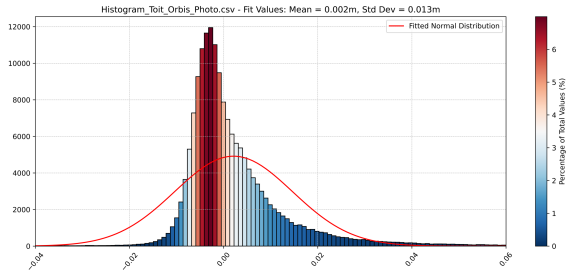

Figure 5. *MMS*-Photogrammetry comparison for the ceiling

Upon closer inspection of the raw data, these higher deviations can be explained by images with higher ISO sensitivity and certain areas being overexposed due to the spotlights distributed across the ceiling. This results in a coarser and more irregular mesh. While detailed analysis of the ceiling beams may not be feasible, the overall dimensions of the structural elements remain measurable.

4.2.3 Analysis of the influence of overexposed areas: Figure 2 clearly shows that very large, bright windows are positioned throughout the room. This results in the appearance of overexposed areas around these windows during image acquisition. Details in these images may no longer be visible and thus will not be present in the mesh. Additionally, the mesh around these areas can be highly irregular in terms of details: if an image is taken from an angle that hides the window and limits overexposure, the details will be much finer compared to images that directly include the windows.

The photogrammetric mesh is much less dense than the *MMS* mesh in this case. If large triangles deviate from the reference,

their influence on the final result will be minimal as only one vertex is used. Thus, the *MMS* mesh is compared to photogrammetry as a reference to better highlight these surfaces that deviate from the *MMS* mesh. This analysis is presented in table 3 and figure 6.

Reference	Compared	*ICP*	Mean	*Std*
Photogrammetry	*Orbis*	0.018	-0.003	0.012

Table 3. Overexposed area comparison

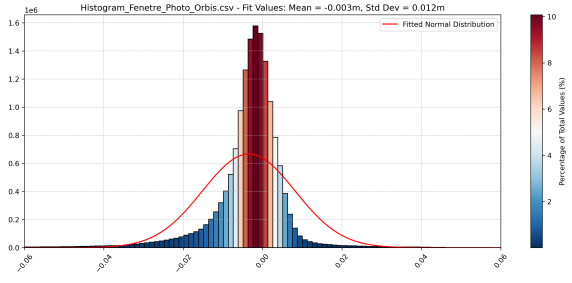

Figure 6. Photogrammetry-*MMS* comparison for the overexposed area

The deviation analysis shows a higher standard deviation compared to previous cases with a similar *GSD*. This directly results from the modelling issues around the overexposed areas in the images. Consequently, in these regions, the photogrammetric mesh deviates much more from the *MMS* mesh. Aside from these significant deviations, the differences remain on the order of a few millimetres, but fine details do not appear in the mesh.

4.3 Conclusion of the geometric analysis

Several cases have been studied, ranging from objects at very short distances to larger and more distant ones. In all cases, hyperfocal focusing allowed for the use of the same optical parameters throughout the acquisition process. It can be concluded that at short distances, the employed method is highly satisfactory, allowing for the creation of a quality mesh that highlights the essential details of surfaces. However, as the distance increases and the focal length remains fixed, the *GSD* also increases, which limits the ability to capture fine details. Nevertheless, the overall structure of the objects is still well-preserved.

Finally, due to the inherent configuration of the room, very bright areas appeared in some images. In these cases, global modelling is still feasible, but care must be taken as modelling errors are more frequent in such conditions.

5. Optimization of the model for 3D rendering

One of the objectives of the Interreg project in which this study is involved is the enhancement of sites through 3D renderings, in the form of individual images or videos, whether in real-time or not. To make this feasible in an optimal way, it is necessary to refine the photogrammetric mesh, specifically by reducing the number of triangles while maintaining a correct topology. Visual details are then simulated using textures applied over the mesh, allowing for a lightweight scene in terms of the number of triangles, but still visually rich.

5.1 Decimation and remeshing

The first crucial step for optimizing 3D renderings is reducing the number of triangles in the mesh. This decimation can be performed in various ways and using different software tools, but in this case, it was done using Meshlab (Cignoni et al., 2008). Several methods were tested, as well as various decimation ratios, to find the best compromise between the number of triangles and visual appearance. The chosen method is the simplification proposed by Garland and Heckbert (1997), implemented directly in Meshlab, resulting in a mesh of 1,250,000 faces instead of the 37 million that composed the original mesh. Next, remeshing was performed using the method proposed by Jakob et al. (2015), resulting in a highly regular mesh with no topological issues.

5.2 Texture application

Since the faces of the mesh were modified, it was necessary to generate a new UV map and apply new textures. A variant of the decimation algorithm was also implemented in Meshlab to compute textures for the new mesh (Garland and Heckbert, 1998). However, when the reduction in the number of faces is substantial, the results were not as good as expected. Textures were then computed in Metashape, and here the result was very satisfactory. The visual rendering is very similar. Additionally, to simulate relief effects on the mesh, normal maps and ambient occlusion maps were generated directly in Metashape from the high-poly mesh.

6. Creation of photorealistic images

The goal of this modelling process is to create 3D renderings that can be viewed by the public. It is essential to ensure a consistent and visually appealing result by replacing poorly reconstructed or missing areas. This step was completed using the free and *open-source* modelling software Blender (2024). Generally, the elements that were modified or modelled were those poorly reconstructed by photogrammetry, especially:

- The floor
- The stairs
- The chandelier, lamps and furniture

For illustration, the example of the chandelier can be taken. It is located in the center of the room and was reconstructed in a highly fragmented manner through photogrammetry. Instead, it was procedurally reconstructed in *Blender*, allowing for adjustments in the positions and rotations of each element to enhance realism, while also making it reusable in another project, with a visually different result by simply adjusting numerical values. This procedural modelling process is presented in more detail by Sommer et al. (2024). The comparison between the two is presented in figure 7.

Similarly, the windows, which appeared very bright in the images, were poorly modelled by photogrammetry. They were also manually modelled afterward. To simulate windows looking outwards, emissive textures were created instead of textures reacting to light. These textures influence the rendering of the interior textures in the throne room, simulating the effects of external conditions on the interior rendering.

Figure 7. Chandelier from photogrammetry and procedurally modelled

By combining photogrammetric and parametric modelling, and using *Blender*'s *Ray-Tracing* rendering tools, high-quality 3D renderings of the throne room can be produced, as shown in figures 8. Additionally, lighting conditions can be varied to simulate different times of day, or objects can be added for a virtual tour of the site.

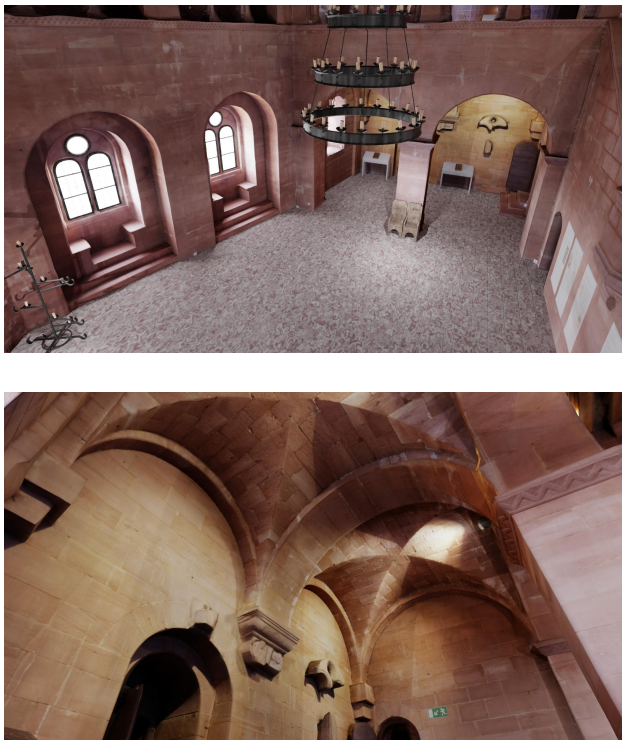

Figure 8. 3D renderings of the throne room

7. Conclusion

The benefits of using hyperfocal distance for photogrammetric modelling has been demonstrated throughout this study. In indoor environments with significant distance constraints, it proves particularly effective in producing consistently sharp images across the entire field, eliminating the need to adjust focus for each situation. Comparison with lasergrammetric data showed minimal discrepancies, ensuring high-quality data acquisition and accurate scaling with known distances used as references. However, as the focal length remains constant throughout the survey, it is essential to strike a balance between *GSD* and field of view, to capture sufficient detail without excessively increasing the final data volume. This also means that for more distant elements, the *GSD* is lower, resulting in less precise and detailed modelling compared to *TLS*. Regarding texture application on the model, the visual result is significantly better with photogrammetry than with *TLS*.

Overall, this method proves particularly effective for this study, whose primary objective is visualization and utilization in 3D environments. It also provides results with good geometric accuracy, although optimal survey conditions are necessary. If further conservation or detailed measurements are required, integrating *TLS* data for the more challenging areas can be highly beneficial. However, as *TLS* equipment is considerably more expensive, this approach is best used to complement the photogrammetric model, ensuring comprehensive, high-quality data across the entire model.

Acknowledgement

We extend our thanks to the "Châteaux Rhénans: Burgen am Oberrhein" Interreg VI Project (2023-2025) involving France, Germany, and Switzerland, coordinated by the European Collectivity of Alsace. We appreciate the opportunity to contribute to this innovative approach to digital heritage conservation.

REFERENCES

Agisoft, 2024. Metashape. `https://www.agisoft.com/`. Online: 2024-11-13.

Barazzetti, L., Previtali, M., Roncoroni, F., 2017. Fisheye Lenses for 3D Modeling: Evaluations and Considerations. *The International Archives of the Photogrammetry, Remote Sensing and Spatial Information Sciences*, XLII-2/W3, 79–84.

Besl, P., McKay, N. D., 1992. A method for registration of 3-D shapes. *IEEE Transactions on Pattern Analysis and Machine Intelligence*, 14(2), 239-256.

Blender, 2024. Blender - a 3d modelling and rendering package. `https://www.blender.org/`. Online: 2024-11-13.

Bruno, N., Perfetti, L., Fassi, F., Roncella, R., 2024. Photogrammetric Survey of Narrow Spaces in Cultural Heritage: Comparison of Two Multi-Camera Approaches. *The International Archives of the Photogrammetry, Remote Sensing and Spatial Information Sciences*, XLVIII-2/W4-2024, 87–94.

Canon, 2024. Profondeur de Champ. `https://www.canon.fr/pro/infobank/depth-of-field/`. Online: 2024-11-13.

Caroti, G., Piemonte, A., Martínez-Espejo Zaragoza, I., Brambilla, G., 2018. Indoor Photogrammetry Using UAVs with Protective Structures: Issues and Precision Tests. *The International Archives of the Photogrammetry, Remote Sensing and Spatial Information Sciences*, XLII-3/W4, 137–142.

Cignoni, P., Callieri, M., Corsini, M., Dellepiane, M., Ganovelli, F., Ranzuglia, G., 2008. MeshLab: an Open-Source Mesh Processing Tool. V. Scarano, R. D. Chiara, U. Erra (eds), *Eurographics Italian Chapter Conference*, The Eurographics Association, 129–136.

CloudCompare, 2024. CloudCompare (version 2.11.3) 3d point cloud and mesh processing software. http://www.cloudcompare.org. Online: 2024-11-13.

Covas, J., Ferreira, V., Mateus, L., 2015. 3D Reconstruction with Fisheye Images Strategies to Survey Complex Heritage Buildings. *Digital Heritage*, 1, 123–126.

Dlesk, A., Vach, K., Holubec, P., 2019. Analysis of Possibilities of Low-Cost Photogrammetry for Interior Mapping. *The International Archives of the Photogrammetry, Remote Sensing and Spatial Information Sciences*, XLII-5/W3, 27–31.

Garland, M., Heckbert, P. S., 1997. Surface simplification using quadric error metrics. *Proceedings of the 24th annual conference on Computer graphics and interactive techniques - SIGGRAPH*, ACM Press, Carnegie Mellon University, 209–216.

Garland, M., Heckbert, P. S., 1998. Simplifying surfaces with color and texture using quadric error metrics. *Proceedings Visualization '98 (Cat. No.98CB36276)*, IEEE, Research Triangle Park, NC, USA, 263–269.

Grussenmeyer, P., Alby, E., Landes, T., Koehl, M., Guillemin, S., Hullo, J. F., Assali, P., Smigiel, E., 2012. Recording Approach of Heritage Sites Based on Merging Point Clouds from High Resolution Photogrammetry and Terrestrial Laser Scanning. *The International Archives of the Photogrammetry, Remote Sensing and Spatial Information Sciences*, XXXIX-B5, 553–558.

Jakob, W., Tarini, M., Panozzo, D., Sorkine-Hornung, O., 2015. Instant Field-Aligned Meshes. *ACM Transactions on Graphics (Proceedings of SIGGRAPH ASIA)*, 34(6), 189–1.

Jordá, F., Navarro, S., Pérez, A., Cachero, R., López, D., Lerma, J. L., 2011. Close range photogrammetry and terrestrial laser scanning: high resolution texturized 3d model of the chapel of the kings in the palencia cathedral as a case study. *Proceedings of the XXIIIrd international CIPA symposium, CTU-CIPA, Prague*.

Kazhdan, M., Bolitho, M., Hoppe, H., 2006. Poisson surface reconstruction. *Proceedings of the fourth Eurographics symposium on Geometry processing*, 7(4).

Kingslake, R., 1992. *Optics in Photography*. SPIE Optical Engineering Press.

Kraus, K., 2007. *Photogrammetry: Geometry from Images and Laser Scans*. De Gruyter Textbook, 2, Walter De Gruyter.

Kulbe, E., 2024. Trifels's throne room. https://burgenlandschaft-pfalz.de/fileadmin/_processed_/9/e/csm_2023_Trifels_018_b8c6ac3e9c.jpg. Online: 2024-11-13.

Lluis i Ginovart, J., Mª Toldrà, J., Costa, A., Coll, S., 2014. Close Range Photogrammetry and Constructive Characterization of Masonry Gothic Vaults. *Revista de la Construcción. Journal of Construction*, 13(1), 47–55.

Luhmann, T., Robson, S., Kyle, S., Boehm, J., 2014. *Close-Range Photogrammetry and 3D Imaging*. 2, De Gruyter, Berlin, Boston.

Marčiš, M., Barták, P., Valaška, D., Fraštia, M., Trhan, O., 2016. Use of Image Based Modelling for Documentation of Intricately Shaped Objects. *The International Archives of the Photogrammetry, Remote Sensing and Spatial Information Sciences*, XLI-B5, 327–334.

Matoušková, E., Pavelka, K., Smolík, T., Pavelka, K., 2021. Earthen Jewish Architecture of Southern Morocco: Documentation of Unfired Brick Synagogues and Mellahs in the Drâa-Tafilalet Region. *Applied Sciences*, 11(4), 1712.

Pavelka, K., Raeva, P., Pavelka jr., K., Kýhos, M., Veselý, Z., 2022. Analysis of Data Joining from Different Instruments for Object Modelling. *The International Archives of the Photogrammetry, Remote Sensing and Spatial Information Sciences*, XLIII-B2-2022, 853–860.

Pfeuffer, U., 2024. Trifels. https://burgenlandschaft-pfalz.de/fileadmin/_processed_/b/e/csm_20190703Trifels05_989b849de0.jpg. Online: 2024-11-13.

Pérez Ramos, A., Robleda Prieto, G., 2015. 3D Virtualization by Close Range Photogrammetry Indoor Gothic Church Apses. The Case Study of Church of San Francisco in Betanzos (La Coruña, Spain). *The International Archives of the Photogrammetry, Remote Sensing and Spatial Information Sciences*, XL-5/W4, 201–206.

Rapuca, A., Matoušková, E., 2023. Testing of Close-Range Photogrammetry and Laser Scanning for Easy Documentation of Historical Objects and Buildings Parts. *Stavební obzor - Civil Engineering Journal*, 32(4), 504–518.

Sammartano, G., Patrucco, G., Avena, M., Bonfanti, C., Spanò, A., 2024. Enhancing Terrestrial Point Clouds Using Upsampling Strategy: First Observation and Test on Faro Flash Technology. *The International Archives of the Photogrammetry, Remote Sensing and Spatial Information Sciences*, XLVIII-2/W4-2024, 381–388.

Sommer, E., Koehl, M., Grussenmeyer, P., 2024. Crafting and Modifying Rhine Castle Models with Parametric Modeling in Blender. *The International Archives of the Photogrammetry, Remote Sensing and Spatial Information Sciences*, XLVIII-2/W4-2024, 405–412.

Spencer, C., 2023. Hyperfocal Distance Explained. https://photographylife.com/hyperfocal-distance-explained. Online: 2024-11-13.

Stubbs, N., 2021. Hyperfocal Distance. https://www.all-things-photography.com/hyperfocal-distance/. Online: 2024-11-13.

Tsiachta, A., Argyrou, P., Tsougas, I., Kladou, M., Ravanidis, P., Kaimaris, D., Georgiadis, C., Georgoula, O., Patias, P., 2024. Multi-Sensor Image and Range-Based Techniques for the Geometric Documentation and the Photorealistic 3D Modeling of Complex Architectural Monuments. *Sensors*, 24(9), 2671.

Vujic, S., Peric, D., Livada, B., 2021. Hyper Focal Distance Application for Long Range Surveillance Camera Zoom Lens Focusing Settings. *IcETRAN 2021*, Ethno Village Stanisici, RS, BIH, 6.